Using cellulose polymorphs for enhanced hydrogen production from photocatalytic reforming.

CHANG, C., SKILLEN, N., NAGARAJAN, S., RALPHS, K., IRVINE, J.T.S., LAWTON, L., ROBERTSON, P.K.J.

2019

Journal Name

COMMUNICATION

Using Cellulose Polymorphs for Enhanced Hydrogen Production from Photocatalytic Reforming

Received 00th January 20xx,
Accepted 00th January 20xx

DOI: 10.1039/x0xx00000x

www.rsc.org/

Colby Chang[a], Nathan Skillen[b]*, Sanjay Nagarajan[b], Kathryn Ralphs[b], John T. S. Irvine[c], Linda Lawton[d] and Peter K. J. Robertson[b]

Efficient energy production and waste valorisation are the most challenging fields in photocatalysis. Reported here is enhanced hydrogen production from cellulose, achieved through the conversion of cellulose I to II *via* a simple pretreatment step.

Photocatalytic conversion of waste material to sustainable fuels is a highly desirable yet challenging process. Specifically, the formation of H_2 over a semiconductor using either water or a sacrificial electron donor (SED) remains one of the biggest challenges in the field of photocatalysis since the initial publication by Fujishima and Honda[1]. Ever since, focus has primarily been on material synthesis to produce a highly active and preferably solar activated catalyst. Alongside this, research into the use of SEDs to facilitate the production of H_2 has also increased. SEDs have been frequently used to supply electrons and reduce recombination by undergoing an irreversible oxidation reaction. SEDs such as methanol, oxalic acid and trimethylamine are among the most commonly reported in the literature[2-4]. More recently, with the increase in bioenergy applications, focus has shifted to cheaper alternative SEDs such as glycerol[5] and lignocellulosic biomass[6]. Both compounds are abundant and have low commercial value making them ideal for photocatalytic applications.

While glycerol has been shown to be readily oxidised and reduced to H_2 *via* favourable stoichiometry[5,7,8], lignocellulosic biomass is a far more challenging starting material. The primary challenge in utilising lignocellulosic biomass is its recalcitrance possessed due to the interlinked cellulose, hemicellulose and lignin. Resourceful cellulose locked within the biomass, when extracted could however be utilised as the feedstock for a variety of purposes including photocatalytic H_2 production. While limited, there are a number of excellent papers that have shown the potential of directly converting cellulose and cellulose based materials to H_2[6,9-12].

While these papers have shown the potential of the application, the crystallinity and insolubility of cellulose remain an issue. These issues could be eliminated by using a pre-treatment step to form a more favourable starting material. Existing methods however, often include harsh conditions and are energy intensive such as steam explosion and acid hydrolysis. An alternative approach is to convert native cellulose (cellulose I) to one of its polymorphs which often have a smaller particle size, increased lattice distance and reduced crystallinity. The literature has reported a number of ways this can be done[13-16] and recently Nagarajan *et al.* reviewed the conversion of cellulose I to II using tetrabutylammonium hydroxide (TBAH) as an energy efficient and environmentally friendly approach[16].

Therefore, reported in this article is the use of TBAH as a pre-treatment step to convert cellulose I to cellulose II for improved photocatalytic reforming to H_2. To date, this is yet to be reported in the literature with previous publications focusing on direct conversion or liquid phase oxidation products. Furthermore, a novel propeller fluidised photo reactor (PFPR) was used to perform the reaction using low power Light Emitting Diodes (LED) to produce an energy efficient method of generating H_2 from cellulose.

The effect of starting feedstock for photocatalytic H_2 production is shown in Figure 1 along with H_2 production from different batches of cellulose II in the inset (Figure 1 (b)). The conversion of cellulose I to cellulose II *via* TBAH treatment resulted in over a 2-fold increase in H_2 yield; rH_2 increased from 0.05 to 0.13 μmol min^{-1}. Under pure water splitting conditions, no H_2 was detected, suggesting it was the reforming of cellulose that was generating H_2. Furthermore, no H_2 was produced in the absence of Pt, TiO_2 and/or light, confirming that the reaction was due to firstly TiO_2 acting as a semiconductor to generate an electron-

[a]*School of Engineering and Applied Science, Princeton University, New Jersey 08544, United States of America*
[b]*School of Chemistry and Chemical Engineering, Queens University Belfast, David Keir Building, Stranmillis Road, Belfast, UK, BT9 5AL*
[c]*School of Pharmacy and Life Science, Sir Ian Wood Building, Robert Gordon University, Aberdeen, AB10 7GJ*
[d]*School of Chemistry, University of St Andrews, St Andrews, Fife, KY16 9ST*
**Email: n.skillen@qub.ac.uk*

†Electronic Supplementary Information (ESI) available: Methodology and Figure S1-S5 See DOI: 10.1039/x0xx00000x

hole pair and secondly, Pt acting as an electron trap for proton reduction to H_2.

Under photocatalytic conditions, the evolution of H_2 from both cellulose I and II was linear with increasing irradiation time suggesting zero order kinetics. Furthermore, good reproducibility was seen for cellulose II conversion to H_2 as indicated by the replicates shown in Figure 1 (a). In contrast, a slightly larger increase between replicates was seen for cellulose I, which may have been due to the varied range of particles present when in suspension. Comparable H_2 production was also achieved when using different batches of cellulose II to demonstrate the reproducibility of the conversion method (Figure 1 (b)). Batches 1, 2 and 3 were all prepared separately from individual batches of cellulose I (particle range of 106 – 212 μm) and fresh TBAH.

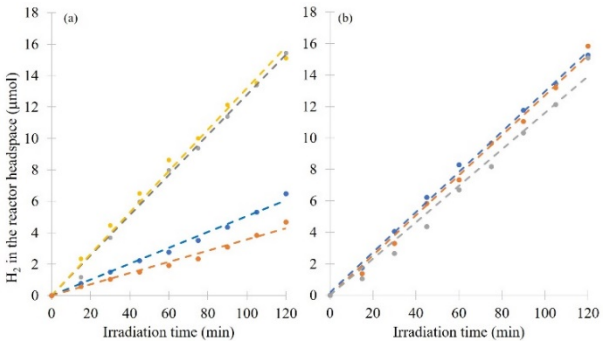

Figure 1. Effect of starting feedstock on photocatalytic H_2 production where (a) shows H_2 from cellulose I (replicate 1 (•) and 2 (•)) and cellulose II (replicate 1 (•) and 2(•)) while (b) is H_2 formation from cellulose II from individually synthesised batches (batch 1 (•), 2 (•) and 3(•))

The improved activity when using cellulose II was also reflected in the overall reaction rates (rH_2) and photonic efficiencies (η_{photon}), Table 1. The data shows over a 2-fold increase for both rH_2 per gram of photocatalyst per hour of irradiation and η_{photon}.

Irradiation Source	rH_2 ($\mu mol\ g_{cat}^{-1}\ hr^{-1}$)	rH_2 max (moles min^{-1})	η_{photon} (%)
Cellulose I	40	1.09×10^{-7}	3.9
Cellulose II	104	2.64×10^{-7}	9.4

Table 1. Calculated H_2 evolution rates per gram of photocatalyst and hour of irradiation and as rH_2 max and η_{photon} (%) for cellulose I and II.

The significantly improved yield when using cellulose II can primarily be attributed to decreased crystallinity, a lower degree of polymerisation, a smaller particle size (see ESI) and an increase in H_2O uptake as a result of increased lattice spacing[16]. The crystallinity of both starting materials was determined from XRD analysis (see ESI)[17]. The X-ray diffractograms showed cellulose I to have typical peaks at 15°, 16.5° and 22.8° while cellulose II was found to have peaks centred around 19.8° and 21.8°, which agreed with the literature[16,17]. The crystallinity of both materials was a crucial factor in the photocatalytic conversion process. The crystallinity of cellulose II was found to be 60 %, which was significantly lower than cellulose I at 85 % (see ESI for calculation). As was also discussed by Caravaca *et al.*, a higher degree of crystallinity results in restricted interaction between the photocatalyst surface and cellulose particles, which is a particular challenge given that both particles were present as a suspension[9]. The cellulose-catalyst interaction was likely the primary parameter which dictated the efficiency of the system. To overcome this limitation, a previous report had used a TiO_2-celullose composite, which created a thin layer of cellulose around TiO_2 particles, which ensured interaction between the two materials[10]. Reported here however, is increased interaction achieved through pre-treatment to decrease the crystallinity of cellulose. Therefore, the observed decrease in crystallinity and rearranged H-bonding network were likely to facilitate an increased interaction between the catalyst particle and the interior sites of cellulose. Furthermore, the increased lattice spacing improved radical diffusion between the planes which broke the glyosidic and hydrogen bonds and accelerated photocatalytic oxidation.

The relationship between cellulose II starting concentration and H_2 production is shown in Figure 2. It was found that increasing the starting concentration in the range of 0.5 – 4 g L^{-1}, resulted in an increase in H_2 while increasing further to 10 g L^{-1} resulted in a 28.5 % drop, Figure 2 (a). As cellulose II was a suspension in the PFPR, increasing to higher loadings had a significant impact on light penetration and at concentration greater than 4 g L^{-1}, the system became saturated. Figure 2 (b) also shows that after 45 – 60 mins of irradiation, steady state H_2 production was achieved for all starting concentrations of cellulose II. A starting concentration of 4 g L^{-1} produced the highest rate of production at ~2.4 μmol hr^{-1} g_{cat}^{-1}. A plot of cellulose II starting concentration versus rH_2 (Figure 2 (c)) and the corresponding natural logarithm plot (Figure 2 (d)) shows that despite an 8-fold increase in cellulose concentration, only a 1.7 fold increase in rH_2 was recorded. This would suggest that the reaction was near zero-order, which was also reported by Caravaca *et al.* when using cellulose I[9].

If a pre-treatment step is used in any photocatalytic application, it is paramount to understand its impact on the overall system. Therefore, to investigate this, cellulose I and II were first washed with distilled H_2O, centrifuged and then filtered (see ESI). The recovered filtrate and 'washed' cellulose were then used as starting feedstocks for photocatalysis. Figure 3 shows the overall effect of the washing steps on H_2 production, which highlights a number of interesting observations (supported by Figure S4 and S5). Firstly, Figure 3 shows the recovered filtrate from both cellulose I and II produced a significant amount of H_2. In particular, cellulose II showed a comparable rH_2 of 0.13 and 0.12 μmol min^{-1} for unwashed cellulose and the recovered filtrate respectively. Furthermore, upon resuspending the washed cellulose, a rH_2 of 0.03 and 0.09 μmol min^{-1} was recorded for cellulose I and II respectively. These findings would suggest that H_2 was forming from both the cellulose particles

and what was potentially being 'washed' off into the recovered filtrate.

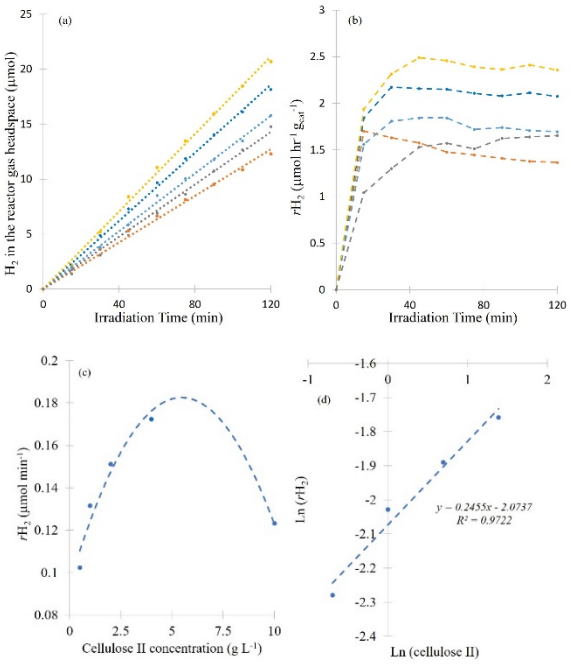

Figure 2. The relationship between cellulose II starting concentration and H_2 production where (a) is the effect of cellulose II starting concentration on H_2 production showing 0.5 (•), 1 (•), 2 (•), 4 (•) and 10 g L^{-1} (•) starting cellulose concentrations, (b) is rH_2 at different starting concentrations, (c) is the plot of rH_2 as a function of cellulose II concentration and (d) is a kinetic plot of Ln (cellulose II) versus Ln (rH_2)

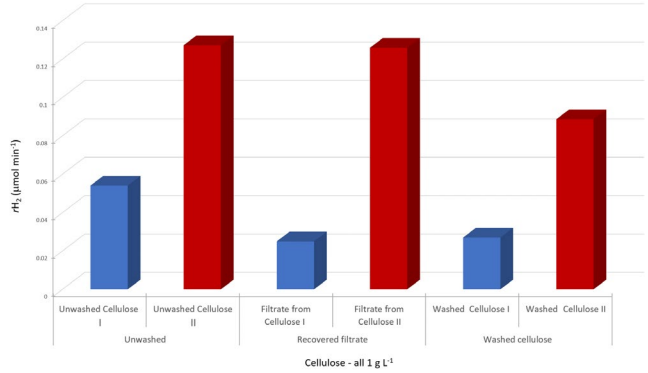

Figure 3. Effect of washing on H_2 production from cellulose; the comparison of cellulose I (■) and II (■) rH_2 when using unwashed cellulose, recovered filtrate (after 1st wash) and washed cellulose (after 1st wash) as a starting feedstock.

In the case of H_2 from cellulose (both washed or unwashed), the likely mechanism was *via* OH• attack which would produce a range of sugars and smaller organic compounds. These compounds would subsequently be readily oxidised in a photocatalytic system, which would also lead to H_2 formation. In the case of the filtrate however, the H_2 may have been coming from either smaller cellulose particles (which passed through the filtering step) or alternatively from smaller dissolved compounds (such as sugars) that had been released during treatment with TBAH. In this instance it would be undesirable to have compounds being released during the pre-treatment stage. To determine if the H_2 formed from the recovered filtrate was due to dissolved organic compounds, HPLC-RI analysis was performed. Samples of the filtrate and of water taken directly from the cellulose II suspension (prior to photocatalysis) showed no products were present in the liquid phase. This confirmed that the pre-treatment step (using TBAH) wasn't releasing any sugars and was facilitating conversion and not hydrolysis. Furthermore, H_2 production was tested using a lower concentration glucose feedstock that corresponded to the limit of detection (LOD) of the HPLC (~ 1 x 10^{-4} g L^{-1}) (Figure S5). Under these conditions, no H_2 was detected which suggests that if any compounds had been released *via* TBAH pre-treatment (that were beyond the LOD of the HPLC), they weren't contributing towards H_2 formation. Based upon these results, the H_2 observed from the washed filtrate was likely forming from smaller cellulose particles that had been released from the washing step and passed through a filtering step (0.22 μm). Particle size analysis (Figure S6 & Table S1) confirmed the presence of smaller particles after filtration in the range of ~ 200 nm, while unfiltered samples showed cellulose II particles to range between 300 and 1842 nm. It was the presence of smaller particles that was thought to contribute towards the formation of H_2.

These observations are further supported by Figure 4 (a) and (b) which show the impact of a second washing step on H_2 production. Figure 4 (a) shows that a second washing step decreased H_2 formation from the recovered filtrate by 65 %, suggesting that the presence of smaller cellulose particles had been reduced. In contrast however, Figure 4 (b) shows that the overall rH_2 from the washed cellulose remained comparable. It is interesting to note that a small induction period occurred when using the washed cellulose II that had been resuspended in H_2O, with linear production occurring after 45 and 60 mins for the 1st and 2nd wash respectively. This was to be expected if the mechanism of H_2 formation is considered to proceed *via* conversion to oxidation products first. As cellulose was present as a suspension, the interaction at the catalyst surface was expected to be low which would reduce initial oxidation and therefore H_2. During the induction period it was likely that cellulose oxidation occurred first, resulting in a build-up of sugars and smaller compounds which subsequently leads to linear H_2 formation (Figure 4 (b)).

The exact mechanism of H_2 formation from cellulose as a SED is yet to be confirmed in the literature. While the mechanism remains elusive, it seems likely that formic acid is expected to be the final intermediate product before conversion to H_2[9]. The pathway from cellulose to formic acid however can proceed *via* multiple mechanisms including OH radical attack of oxidised products [18] as well as the formation of glucose radicals[11]. In the present work the mechanism of formation is still under investigation, with focus now on the determination of various liquid phase products using HPLC analysis. In general, the authors believe the mechanism would follow the pathway detailed in Equations 1-5 and Figure 5, in which cellulose is first

oxidised to glucose and oligosaccharides and a range of glucose oxidation products. Following this, the products are expected to subsequently undergo further OH radical attack leading eventually to mineralisation to H_2 and CO_2.

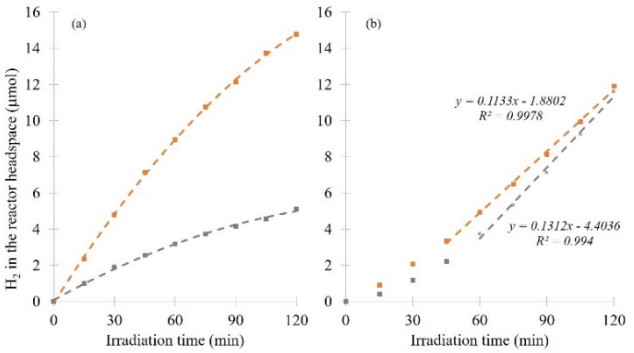

Figure 4. Effect of washing steps on H_2 production from cellulose where (a) shows the effect of the 1st (■) and 2nd (■) wash on H_2 production using the recovered filtrate and (b) the washed cellulose II.

Equation 1 $$Pt - TiO_2 + hv = VB_{h^+} + CB_{e^-}$$

Equation 2 $$VB_{h^+} + OH^- \xrightarrow{TiO_2} OH\bullet$$

Equation 3 $$(C_6H_{10}O_5)_n + OH\bullet + h^+ \xrightarrow{TiO_2} nC_6H_{12}O_6$$

Equation 4 $$C_6H_{12}O_6 + OH\bullet \xrightarrow{TiO_2} Ox_{product} + H^+$$

Equation 5 $$H^+ + 2e^- \xrightarrow{Pt} H_2$$

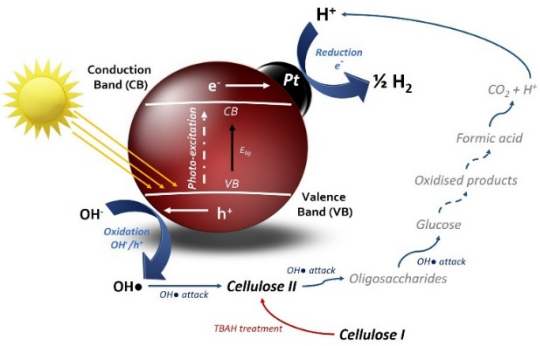

Figure 5. Illustration of the proposed mechanism of cellulose II photocatalytic reforming to H_2

Conclusion

The conversion of cellulose I to cellulose II *via* a TBAH pre-treatment step has been found to be favourable for photocatalytic reforming to H_2. Using cellulose II, a 2-fold increase in rH_2 over cellulose I was recorded along with an increase in photonic efficiency from 3.9 to 9.4 % in an LED irradiated PFPR. Pre-washing both cellulose materials also showed that smaller particles were released that could primarily contribute towards H_2 formation. Upon resuspending washed cellulose particles into water, an induction period was noted before linear H_2 production occurred. This suggests the mechanism was proceeding *via* initial oxidation to oligosaccharides, smaller sugars and organic compounds before reduction to H_2. These findings are key to further show the potential of photocatalytic technology for the conversion of cellulose to H_2 along with applications in the wider field of bioenergy.

Acknowledgments

Mr Colby Chang would like to acknowledge the International Intern Aboard Program at Princeton University and Queens University Belfast (QUB) for funding his internship. Dr Sanjay Nagarajan would like to acknowledge QUB for funding his research while Dr Nathan Skillen would like to acknowledge the Pioneering Research Program at QUB for funding his research.

References

1 Fujishima, A. and Honda, K., *Nature,* 1972, 238, 37-38.

2 X. Zheng, L. Wei, Z. Zhang, Q. Jiang, Y. Wei, B. Xie and M. Wei, *Int J Hydrogen Energy*. 34 (2009) 9033-9041.

3 N. Skillen, M. Adams, C. McCullagh, S. Y. Ryu, F. Fina, M. R. Hoffmann, J. T. S. Irvine and P. K. J. Robertson, *Chemical Engineering Journal. 286 (2016) 610-621.*

4 X. Xu, G. Liu, C. Randorn and J. T. S. Irvine, *Int J Hydrogen Energy,* 2011, 36, 13501-13507.

5 M. R. K. Estahbanati, M. Feilizadeh and M. C. Iliuta, *Applied Catalysis B: Environmental. 209 (2017) 483-492.*.

6 D. W. Wakerley, M. F. Kuehnel, K. L. Orchard, K. H. Ly, T. E. Rosser and E. Reisner, *Nature Energy,* 2017, 2, 17021.

7 M. Bowker, P. R. Davies and L. Al-Mazroai, *Catalysis Letters,* 2008, 128, 253

8 X. Jiang, X. Fu, L. Zhang, S. Meng and S. Chen, *J. Mater. Chem. A,* 2015, 3, 2271-2282

9 A. Caravaca, W. Jones, C. Hardacre and M. Bowker, *Proceedings of the Royal Society A: Mathematical, Physical and Engineering Science,* 2016, 472.

10 G. Zhang, C. Ni, X. Huang, A. Welgamage, L. A. Lawton, P. K. J. Robertson and J. T. S. Irvine, *Chem. Commun.,* 2016, 52, 1673-1676

11 X. Fu, J. Long, X. Wang, D. Y. C. Leung, Z. Ding, L. Wu, Z. Zhang, Z. Li and X. Fu, *Int J Hydrogen Energy*, 33 (2008) 6484-6491.

12 T. Kawai and T. Sakata, *Nature,* 1980, 286, 474.

13 L. Alves, B. F. Medronho, F. E. Antunes, A. Romano, M. G. Miguel and B. Lindman, *Colloids and Surfaces A: Physicochemical and Engineering Aspects. 483 (2015) 257-263.*

14 E. Jin, J. Guo, F. Yang, Y. Zhu, J. Song, Y. Jin and O. J. Rojas, *Carbohydrate Polymers. 143 (2016) 327-335.*

15 S. Kuga, S. Takagi and R. M. Brown, *Polymer. 34 (1993) 3293-3297.*

16 S. Nagarajan, N. C. Skillen, J. T. S. Irvine, L. A. Lawton and P. K. J. Robertson, *Renewable and Sustainable Energy Reviews. 77 (2017) 182-192.*

17 Segal, L., J.J. Creely, A.E. Martin, and C.M. Conrad*, Textile Research Journal 29, 10 (1959): 786–94.*

18 R. Chong, J. Li, Y. Ma, B. Zhang, H. Han and C. Li, *Journal of Catalysis. 314 (2014) 101-108.*

Conflicts of interest

There are no conflicts to declare.

Electronic Supplementary Information (ESI)

Using Cellulose Polymorphs for Enhanced Hydrogen Production from Photocatalytic Reforming

Colby Chang[a], Nathan Skillen[b], Sanjay Nagarajan[b], Kathryn Ralphs[b], John T. S. Irvine[c], Linda Lawton[d], and Peter K. J. Robertson[b]*

*email: n.skillen@qub.ac.uk phone: 028 9097 5605

[a] *School of Engineering and Applied Science, Princeton University, New Jersey 08544, United States of America*

[b] *School of Chemistry and Chemical Engineering, Queen's University Belfast, David Keir Building, Stranmillis Road, Belfast BT9 5AG, Northern Ireland, United Kingdom.*

[c] *School of Pharmacy and Life Science, Sir Ian Wood Building, Robert Gordon University, Aberdeen, AB10 7GJ*

[d] *School of Chemistry, University of St Andrews, St Andrews, Fife, KY16 9ST*

Number of Pages: 8

Number of Figures: 6

Number of Tables: 1

Supplementary Information

Methods

Cellulose preparation

Cellulose II was prepared from cellulose I using the following method. Briefly, a required quantity of cellulose I (microcrystalline cellulose procured from Acros organics) was separated into different size fractions using sieves with a pore size ranging from 110 to 425 µm (Sigma Aldrich). A predetermined quantity of cellulose I within the size range of 106 – 212 µm was added slowly to a glass vial containing TBAH (55 wt% TBAH in water procured from Alfa Aesar, used as received) and a magnetic stirrer bar to achieve a final concentration of 50 g L^{-1}. The mixture was stirred at room temperature until cellulose I was fully dissolved. Upon complete dissolution, excess anti-solvent (distilled water, at least 300 ml) was added to the mixture with continuous stirring. Cellulose II started to precipitate from solution instantly, however stirring was continued for at least 30 minutes to displace all cellulose. Precipitated cellulose II was filtered using filter paper and then washed with distilled water to remove any bound TBAH and to achieve a neutral pH. Images of the cellulose I and II in suspension (before and after agitation) are shown in Figure S1. Cellulose II was stored in its hydrate form for further experiments. Cellulose II was characterised using XRD to confirm the complete conversion of cellulose I to cellulose II. Crystallinity and lattice distance of both the feedstock were also calculated from the XRD results. The XRD measurements in this work were carried out on a PANanalytical X'Pert Pro X-ray diffractometer. The X-ray source was copper with a wavelength of 1.5405 Å. All measurements were carried out ex-situ using a spinning stage. The diffractograms were recorded from 4° to 50° with a step size of 0.017°. Particle size analysis was performed on cellulose 2 samples using a Malvern Zetasizer (Nanoseries, Nano-ZS) for unwashed and washed filtered samples. Unwashed samples were diluted with H_2O where required prior to analysis, while filtered samples were passed through a 0.22 µm syringe filter.

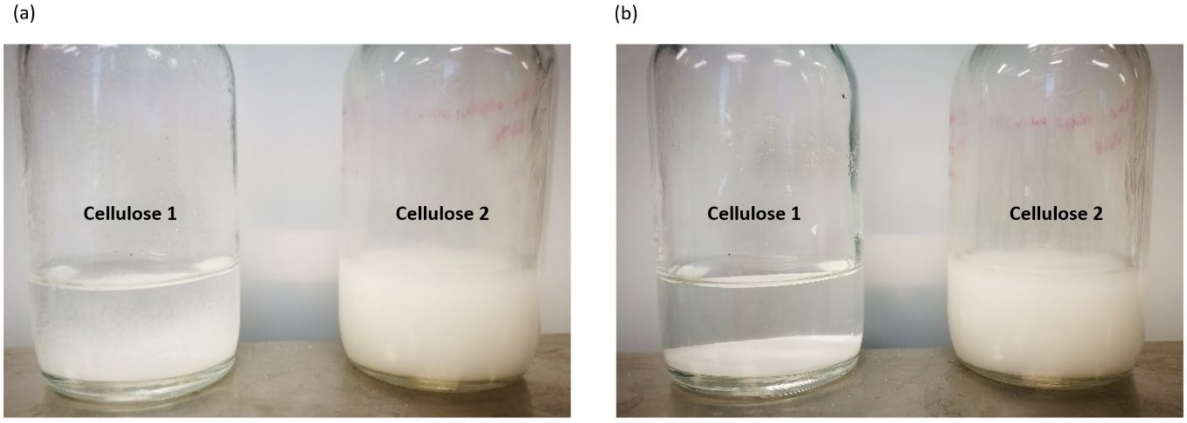

Figure S1**.** images of cellulose I and II agitated suspensions (a) and after 30 seconds of settling

Reactor concept and photocatalytic procedure

The reaction was performed in the PFPR, which is an annular glass bodied reactor that uses a stainless steel 4-blade propeller to create fluidisation. Full details of the reactor can be found elsewhere[1], however in general, the PFPR was operated as a sealed batch unit, with a propeller rotation speed of 1200 rpm. The reaction was performed under a N_2 atmosphere, with the PFPR being purged for 15 mins (150 mL min^{-1}) prior to any irradiation being switched on. Irradiation was provided by a novel spiral jacket array constructed from UV-LEDs (Lighting Will), which provided 360° irradiation of the PFPR. The LEDs had a peak wavelength in the range of 365 – 370 nm and were operated at V_F = 12.0 dcV and I_F = 1.1 A, which gave an overall electrical power of 13.2 W. Figure S2 (a) shows the PFPR under irradiation from the UV-LED cylindrical jacket while Figure S2 (b) and (c) shows the thermal imaging of the PFPR and LED array (Model TG165, FLIR). The LED jacket had a temperature of 39.5°C when operating, while the reaction solution inside the PFPR was at 28.5°C.

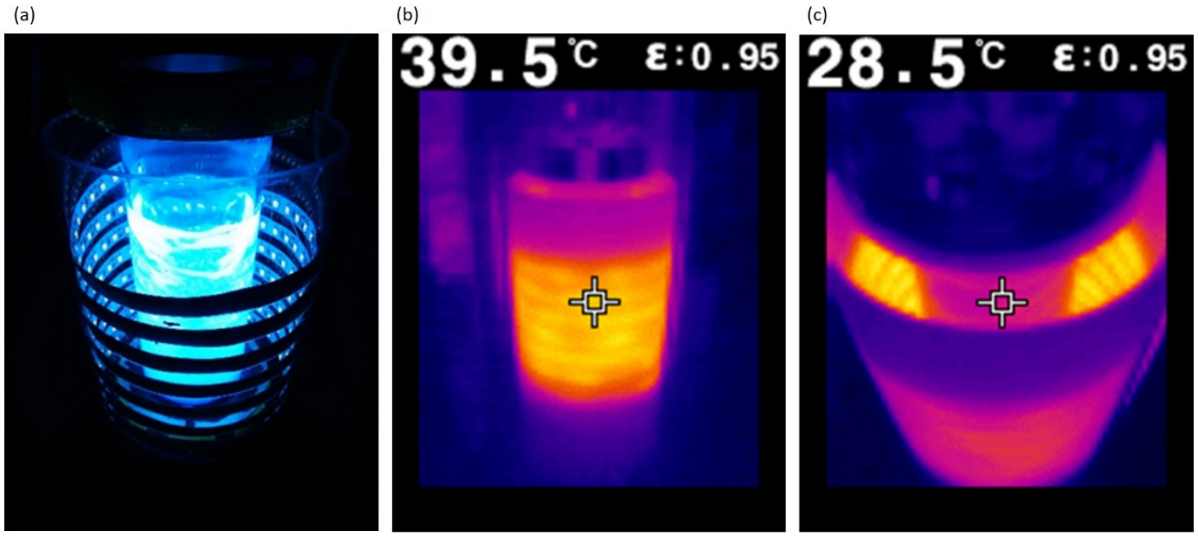

Figure S2. (a) image of the PFPR under irradiation (quinine was used for illustration purposes only) from the UV-LED cylindrical jacket array, (b) thermal image of the PFPR under irradiation and (c) thermal image of the reaction solution inside the PFFR while under irradiation

The intensity of the array was measured using actinometry and the potassium ferrioxalate method, which gave a value of 2.81 x 10^{-6} moles of photons min^{-1} (Equation S1 and S2). The array was also measured used a radiometer (UV-X) and gave an intensity of 5 mW cm^{-2} when the probe was positioned at the centre of the cylindrical array (4.5 cm away from the LED jacket array).

Equation S1 $$Photon\ flux = \frac{Moles\ of\ Fe^{2+}}{\sigma Fe^{2+} x\ t}$$

Where 'moles of Fe^{2+}' were determined based on the potassium ferrioxalate method (7.68 x 10^{-6}), 'σFe^{2+}' was set at 0.97 and 't' was the time (min) the actinometry solution was irradiated for. The photonic efficiency was then determined based on the calculated photon flux (2.81 x 10^{-6} mole of photons min^{-1}) and Equation S2.

Equation S2 $$\eta_{photon}(\%) = \frac{2\ x\ rH_2\ (moles\ of\ H_2\ min^{-1})}{photon\ flux\ (mole\ of\ photons\ min^{-1})} x\ 100$$

Where, 'η_{photon} (%)' is the photonic efficiency, 'rH_2' is the H_2 formation rate as moles per min and 'photon flux' is the mole of photons entering the reactor per min, as determined by actinometry. As H_2 formation is a 2-electron step, the $_rH_2$ was multiplied by 2.

In a typical experiment, 100 mL of distilled water was used as the reaction solvent with a set loading of cellulose and catalyst added. Cellulose in the range of 0.5 - 4 g L^{-1} was used while the catalyst remained constant at 0.75 g L^{-1}. The catalyst used throughout the investigation was TiO_2 (Hombikat) with a 0.5 % wt. Pt co-catalyst loading (herein referred to as 0.5 % Pt-TiO_2), synthesised via wet impregnation. Briefly, platinum nitrate was mixed with distilled water to match the number of pores of TiO_2. This was then added to TiO_2 in three portions and mixed until the catalyst was homogeneous. The catalyst was then dried over a period of 4 hours at 120 °C and finally calcined for a further 4 hours at 500 °C.

Washed Cellulose Samples

In addition to using cellulose I and II as starting feedstocks, experiments using washed and recovered filtrate samples were also performed. To obtain washed samples, cellulose I and II particles were washed in typically 100 mL volumes of distilled H_2O for a predetermined amount of time. These were performed under dark conditions in clean glass beakers with no presence of TBAH and/or any photocatalyst. The reaction suspension was then filtered to separate the suspended cellulose particles and the filtrate. The cellulose particles were resuspended in fresh H_2O (referred to as *'washed cellulose'*) and run under photocatalytic conditions (addition of Pt-TiO_2). The filtrate (referred to as *'recovered filtrate'*) was also run under photocatalytic conditions, by the addition of only Pt-TiO_2 (no

added cellulose). Experiments were also performed where the above procedure was repeated, which was referred to as a 2nd wash.

Analysis

Samples (0.1 mL) were taken at dedicated time intervals from the PFPR gas headspace (100 mL) and analysed using a gas chromatography (GC) system equipped with a thermal conductivity detector (TCD). An Agilent Technologies 7280 A GC system, hosting a packed column (RESTEK, 2 mm ID) was used. The injector was operated at a temperature of 150 °C, pressure of 26.1 psi and a flow rate of 22.9 mL min^{-1}. The flow rate in the column was 20 mL min-1 with an oven temperature of 50 °C, while the detector was maintained at 200 °C with a flow rate of 5 mL min^{-1}. Ar was used as the carrier gas. H_2 was determined by comparison to a standard injection of pure H_2, while quantification was determined form a calibration of known concentrations.

Liquid phase sample were analysed using an Agilent 1260 infinity high performance liquid chromatography system equipped with a refractive index detector (HPLC-RI) and hosting a Rezex ROA-Organic acid H+ column (300 × 7.8 mm). The mobile phase (5 mM H_2SO_4) flow rate was set at 0.5 mL min^{-1} and a sample volume of 10 µl was withdrawn to analyse for products. RI and column temperatures were set to 40 °C. HPLC profiles of the various commercial standards (including oligo and monosaccharides and a range of sugar oxidation products) were obtained and a calibration curve was prepared against which the unknown samples were measured.

Equation S3 $\quad CrI \text{ for cellulose I} = \frac{(I_{(200)} - I_{amI})}{I_{(200)}} \times 100$

Equation S4 $\quad CrI \text{ for cellulose II} = \frac{(I_{(1-1\,0)} - I_{amII})}{I_{(1-1\,0)}} \times 100$

Where CrI (%) is the crystallinity index (%) of cellulose, $I_{(200)}$ is the intensity of cellulose I at 2θ = 22.5°, I_{amI} is the intensity of cellulose I at 2θ = 18°, $I_{(1\text{-}1\,0)}$ is the intensity of cellulose II at 2θ = 19.8° and I_{amII} is the intensity of cellulose II at 2θ = 16°.

Supplementary Information Results

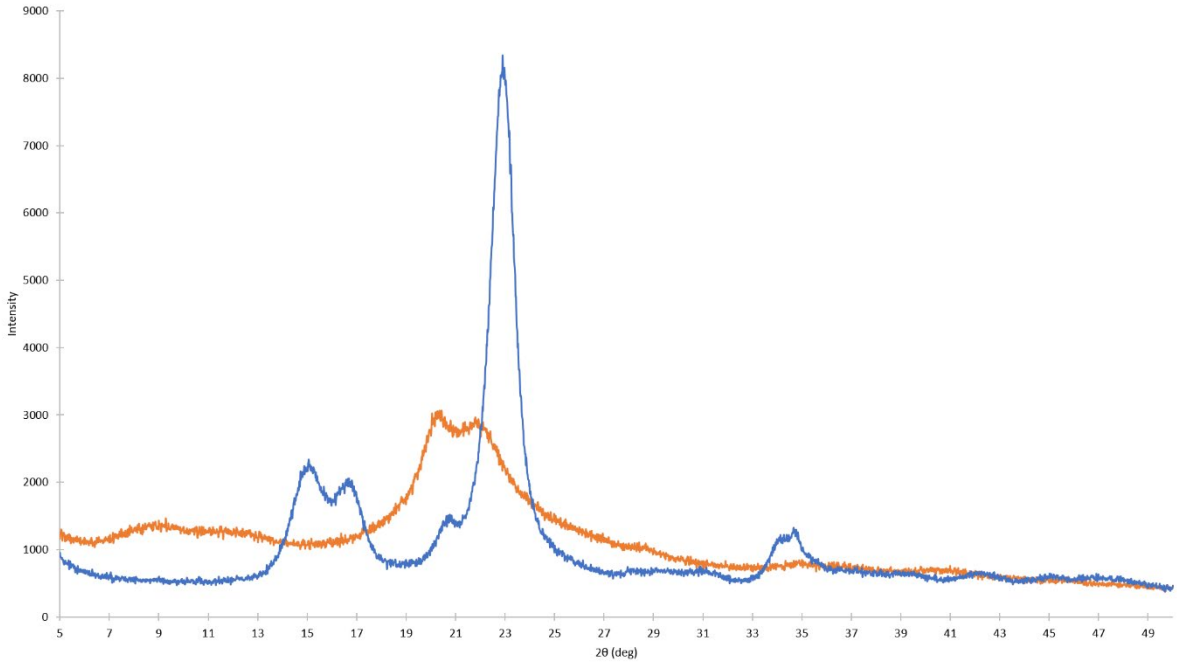

Figure S3. XRD pattern of cellulose I (•) and II (•) samples

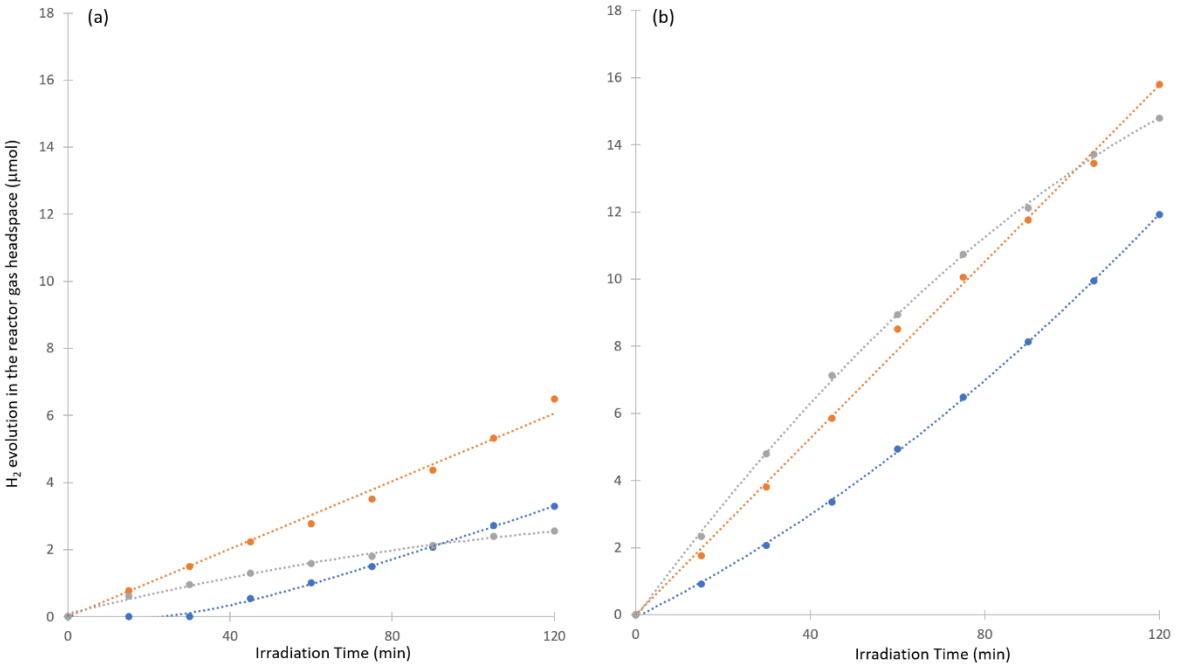

Figure S4. H_2 formation as a function of irradiation time from (a) cellulose I and (b) cellulose II where (•) is unwashed cellulose, (•) is washed cellulose and (•) is the recovered filtrate from washing

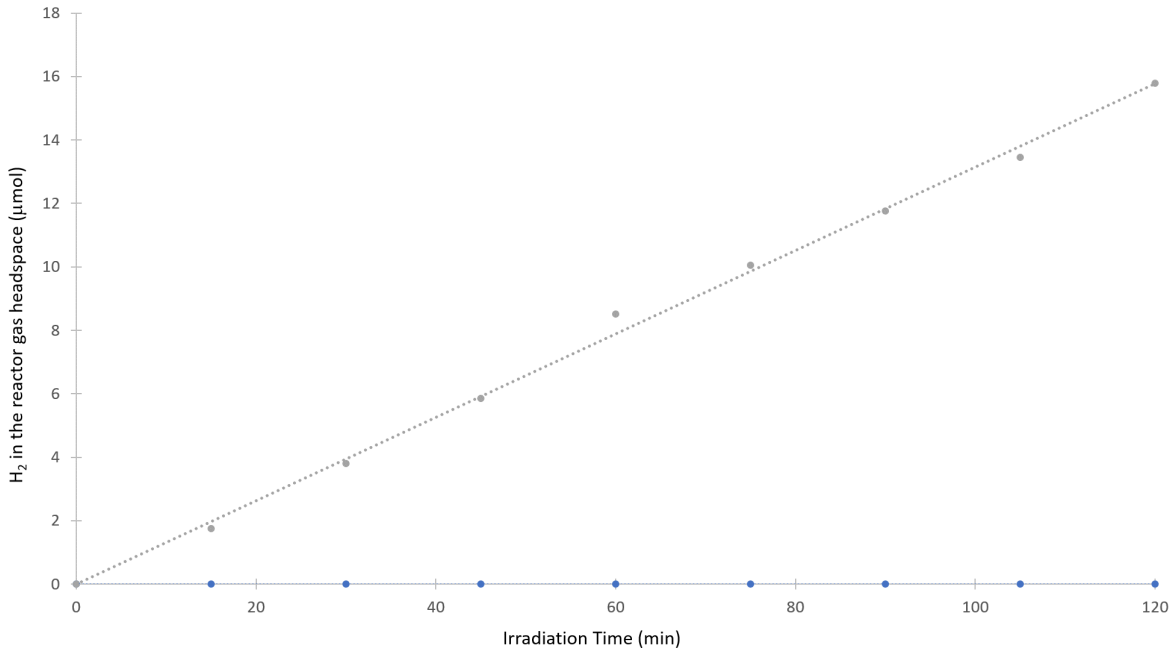

Figure S5. H_2 formation as a function of irradiation time from cellulose II at 1 g L^{-1} (•) and glucose at 1 x 10^{-4} g L^{-1} (•)

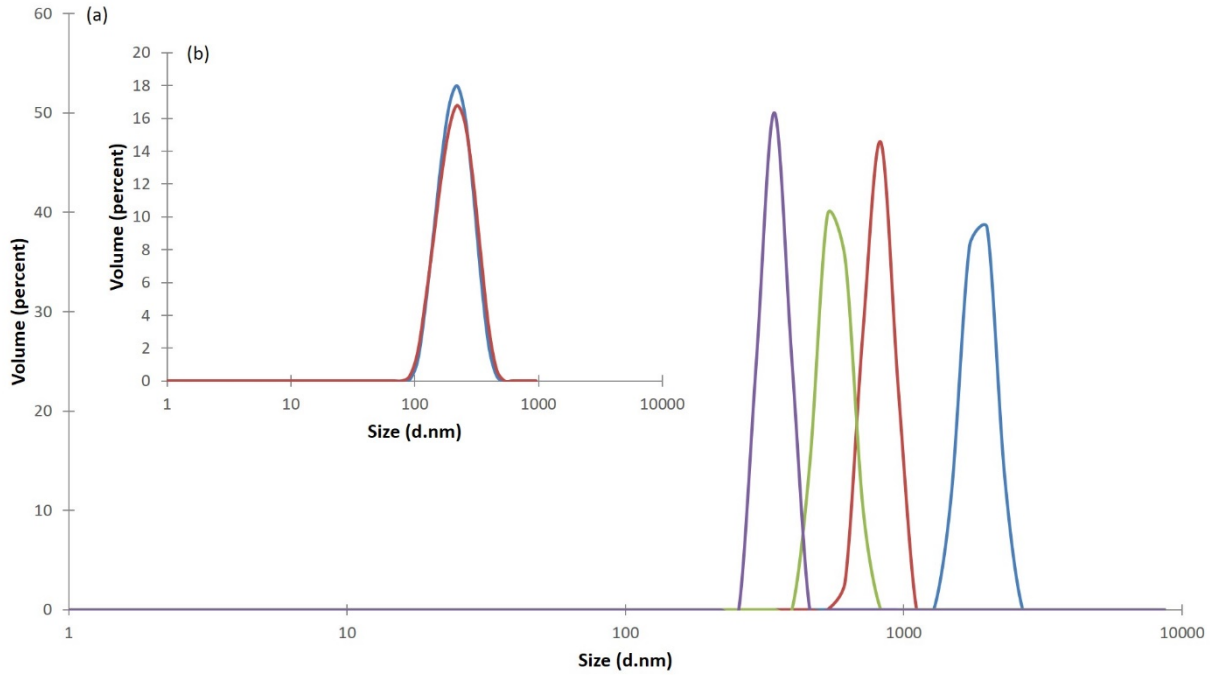

Figure S6. Particle size analysis of cellulose II samples where (a) is unfiltered samples for a 1:2 dilution (•), 1:4 dilution (•), 1:8 dilution (•) and 1:16 dilution (•) from a concentrated stock solution and (b) is filtered samples through a 0.22 μm filter for two replicate samples (replicate 1 (•) and replicate 2 (•))

Cellulose Sample	Mean Particle size (nm)
Cellulose II (unfiltered) – 1:2 dilution	*1847*
Cellulose II (unfiltered) – 1:4 dilution	*808.9*
Cellulose II (unfiltered) – 1:8 dilution	*562.1*
Cellulose II (unfiltered) – 1:16 dilution	*342*
Cellulose II (0.22 μm filtered) - replicate 1	*215.3*
Cellulose II (0.22 μm filtered) - replicate 2	*219.1*

Table S1. Particle size analysis of cellulose 2 samples unfiltered and 0.22 μm filtered. Unfiltered samples were diluted with water to provide an accurate reading for the instrument

References

[1] N. Skillen, M. Adams, C. McCullagh, S. Y. Ryu, F. Fina, M. R. Hoffmann, J. T. S. Irvine and P. K. J. Robertson, *Chemical Engineering Journal*. 286 (2016) 610-621.